Indonesian Journal of Electrical Engineering and Computer Science
Vol. 32, No. 1, October 2023, pp. 52∼60
ISSN: 2502-4752, DOI: 10.11591/ijeecs.v32i1.pp52-60

Analysis of a field oriented control based variable direct current link drive for electric vehicles

Muhammad Helal Uddin, Sharith Dhar, Asif Mohammed Siddiqee, Rahul Chowdhury, Akramul Haque, Mohammed Saifuddin Munna
Department of Electrical and Electronic Engineering, Faculty of Engineering, Premier University, Chattogram, Bangladesh

Article Info

Article history:

Received Mar 14, 2022
Revised Jun 10, 2023
Accepted Jun 17, 2023

Keywords:

Electric vehicles
Field oriented control
Permanent magnet machine
Power converters
Power efficiency

ABSTRACT

The performance and efficiency of electric vehicles (EVs) depend mostly on the EVs powertrains. Therefore, one of the most vital research areas is the efficiency analysis of the drivetrain parts in electric vehicles. In this work, two basic drivetrain configurations of EVs are considered and evaluated. Firstly, the one with constant direct current (DC) link voltage and second one having a bidirectional DC-DC converter which supplies variable DC link voltage to the inverter. In order to control a permanent magnet synchronous machine (PMSM), field oriented control (FOC) technique is performed. Furthermore, a bidirectional DC-DC converter with optimized parameters is designed and implemented with variable DC link voltage controller. Finally, a comparison is made taking into account both drivetrain configurations with details efficiency analysis using real time switches at wide operating points of the machine.

Corresponding Author:

Muhammad Helal Uddin
Department of Electrical and Electronic Engineering, Faculty of Engineering, Premier University
1/A, O.R. Nizam Road, Prabartak Circle, Chattogram 4203, Bangladesh
Email: helal_eee@puc.ac.bd

1. INTRODUCTION

Considering the alarming rate of depletion of fuel reserve and due to arising concerns about the global climate change, the conventional transportation systems open to many problems nowadays. The power and energy sector accounts for a large share of worldwide emissions, which accounts for 40% of worldwide CO_2 production followed by the transportation sector (24%) [1], [2]. This motivates researchers to develop sustainable transportation means as top priorities. There has been increased research in the research and development (R&D) area of electric vehicles (EVs) due to the government policies like zero-emission vehicle (ZEV) convention in the USA, China, and Canada [3]. It is estimated that by 2030, electric vehicles will be 30% of the total vehicles on the road [4], [5]. Many of the big cities in the world are seeing the transition to electric vehicles as a prospective solution to improving local air quality, diminishing climate changes and rising the economies.

The major subsystems of an EV is the electric propulsion systems. Selection of traction motors can be choosen depending on three factors efficiency, reliability and cost. The manufacturers adopt four major types of electric motors which include the direct current (DC) motor, induction motor (IM), permanent magnet synchronous machine (PMSM), and switched reluctance machine (SRM). PMSM machine poses high power density, high torque density, high efficiency over a wide range of speed but reasonably high cost [6]. Hence, to reduce the cost non permanent magnet (PM) machine are the potential candidate of PM based machine. Because of the reliability, roughness and low cost of IM, they are well suited for traction and industrial applications [7]. Most of the researchers are working on optimizing PMSM and IM according to the major requirements in EVs electric traction system [8], [9]. Meanwhile, SRM is becoming more popular and recognized as having potential benefits from simple structure, easy control and excellent torque speed characteristics [10]. In order to get good dynamic response and efficiency, it is challenging task to select proper control strategy for PMSM. There are mainly two control aspects: field oriented control (FOC) and direct torque control (DTC). Despite of having simple structure and faster control, DTC has high current and torque ripple [11]. On the contrary, FOC allows decoupling between flux and torque and thus can cover wide speed range but control strategy is complex. Therefore, there is no straight answer of the question about superior technique between FOC and DTC.

EVs drivetrain configurations is another essentials aspect. There are two possible powertrain configuartions; the first one includes an energy source, an inverter and the motor and the second configuration has a bidirectional DC-DC converter in between energy source and inverter [12]. The purpose of this DC-DC converter is to provide variable DC link voltage (V_{dc}) based on driving cycle requirements [13], [14]. This bidirectional DC-DC converter not only decreases inverter stress but also improves the motor performance by regulating system voltage without raising battery costs and size, despite having higher cell number requirements [15], [16]. However, in spite of the decrease in battery size, this DC-DC converter has power losses. Hence, optimization of inductor and power switches must taken into account during design. Lots of research suggested and assessed bidirectional DC-DC converters for EVs and most of them offered a comparison of efficiency but mainly for fixed input and output parameters [17]. Dusmez *et al.* [17] proposes a three level nonisolated bidirectional DC-DC converter which reduces the size of magnetic components and exhibits considerable efficiency improvement compared to two level converter under available driving cycle conditions. Many pieces of research are going on wide band gap material (silicon carbide (SiC) and gallium nitride (GaN)) based DC-DC converters. SiC-based converter provides much better mileage per energy converted, volume reduction and less need of cooling due to the device losses reduction [18].

In order to enhance the efficiency of DC-DC converter, three phase inverter and PMSM, PMSM motor drive topology based on variable V_{dc} link is effective. Different DC-DC converter topologies and their control methods for PMSM based drivetrains for the practical realization of V_{dc} are outlined in [19]. An online method is proposed to calculate the required DC link voltage in low speed operating region of machine which performs higher efficiency due to lower switching losses in the inverter [20]. Prabhakar *et al.* [20] developed a method to optimize V_{dc} for wide speed variations a maximum torque per ampere criteria based on offline calculation method. There have been various works on the effective assessment of EV drivetrains so far. However, most of the works confined to evaluate DC-DC converter performance optimization not overall systems performance and some only considers limited torque and speed range. Following of this flow, we have tried to evaluate the performance and efficiency of EVs using full bridge (four legs) bidirectional DC-DC converter and PMSM motor through FOC controller and DC link voltage controller implementation.

2. DRIVETRAIN AND CONTROLLER STRATEGY

Two drivetrains is considered in this work, one is without DC-DC converter $(C1)$ and another is with inclusion of DC-DC converter $(C2)$ as shown in Figure 1. In Figure 2, field oriented control (FOC) is performed with DC link voltage controller. In DC link controllers there are an inner current loop to control the inductor current in addition with an outer voltage controller to control the voltage across DC link capacitor.

In order to regulate the d-axis and q-axis current two proportional-integral (PI) regulators are used. The PI current controllers correct the error difference between d, q projections of the stator phase currents to their reference values d-axis current and q-axis current. Then the outputs of the current controllers passed through inverse park transformation and using the pulse width modulation (PWM) technique a new stator voltage vector is obtained to the motor (Figure 2). The q- axis reference current will be calculated from torque reference and is proportional to the torque demand. It is not possible to control d and q-axis current independently due to the cross coupling effects such as presence of $\omega_e L_q i_q$ and $\omega_e L_d i_d$ terms. These effects become dominated as speed increases. Hence, it is necessary to compensate the cross coupling effects else it will affect current responses as well as torque response in the high speed operating region. Hence, feed forward compensation is implemented.

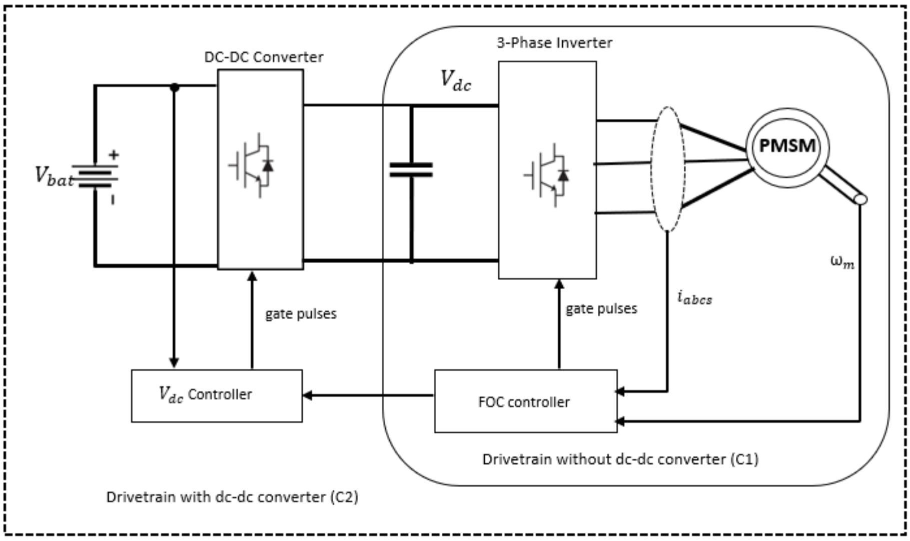

Figure 1. Drivetrain configurations C1 and C2

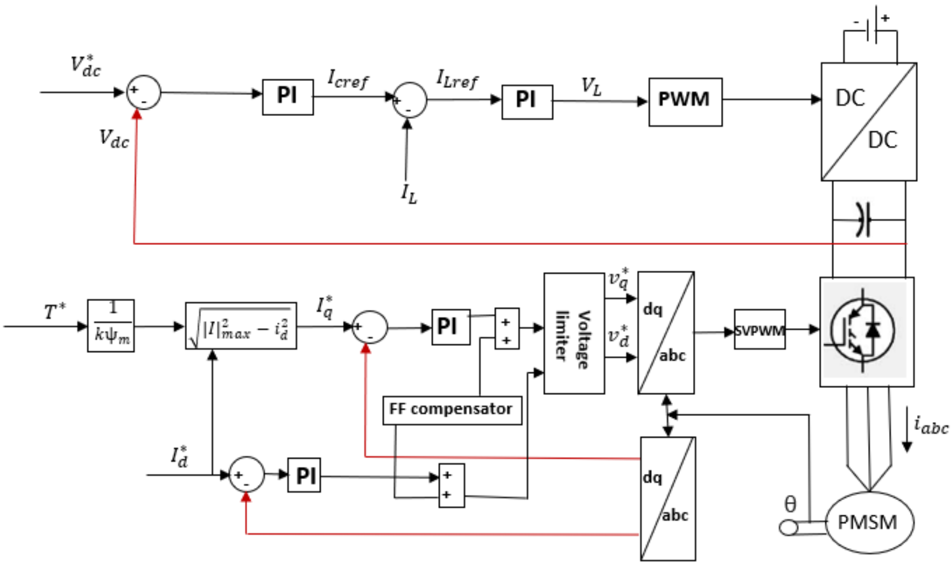

Figure 2. Control strategy with variable DC link voltage controller

2.1. d-q reference model of PMSM

For the ease of control purpose, three phase model of PMSM can be represented in d-q axis frame by applying (ψ_m) whereas q-axis bisects the section between permanent magnets. As the magnet is embedded in the rotor, the magnet flux rotated with the rotor's speed as well as the stator's magnetic flux. I_q currents creates mmf in q-direction called torque current. Similarly, I_d currents create mmf in the d-direction called the field current. The voltage across d and q axis as (1) and (2).

$$v_d = R_s i_d + L_d \frac{di_d}{dt} - \omega_r L_q i_q \quad (1)$$

$$v_q = R_s i_q + L_q \frac{di_q}{dt} + \omega_r L_d i_d + \omega_r \psi_m \quad (2)$$

3. CONTROL PRINCIPLE OF PMSM

The PMSM machine drive features depict in Figure 3. It is shown from Figure 3(a), that PMSM provide a steady torque up to the base speed and then provide peak torque that is inversely proportional to the maximum speed. For operating machines up to base speed either i_d kept zero or maxium torque per ampere (MTPA) strategy is applied. Beyond base speed field weakening (FW) control is implemented.

3.1. Current and voltage limits

The maximum current limit of a machine depends on the power rating of the inverter and machine's maximum thermal limit can be represented as (3).

$$I_s = \sqrt{i_d^2 + i_q^2} \leq I_{max} \tag{3}$$

It can be seen from Figure 3(b), a circle can be formed in the i_d-i_q plane with the fixed radius of i_{max} which is the machine's maximum peak current limit and independent of the machines speed.

The voltage limit V_{max} for the inverter rely on the DC link voltage V_{dc} and the machine insulation. This voltage is restricted to the range $V_{dc}/\sqrt{3}$ [21]. Meanwhile, this secures the existence of voltage rotating vector inside the maximum voltage limit. This voltage limit can be portrayed by ellipses which radius become smaller with the increase in machine's rotational speed. The centre of this ellipses can be denoted by the point $(-\psi_f/L_d, 0)$ known as the critical current in the i_d-i_q plane as presented in Figure 3(b). The voltage limit can be represented as (4).

$$V_s = \sqrt{v_d^2 + v_q^2} \leq V_{max} \tag{4}$$

Where V_{max} is the inverter's highest available output voltage depending on the DC bus voltage.

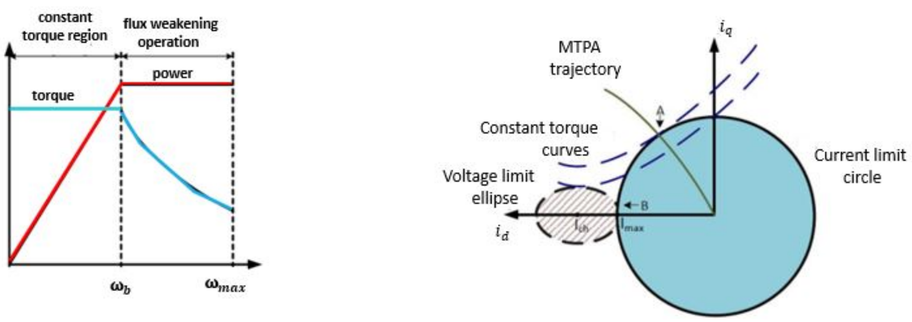

(a) (b)

Figure 3. PMSM drive characteristics (a) operating region and (b) current limit circle and voltage limit ellipse

4. DC LINK VOLTAGE CONTROLLER

The function of the DC link voltage controller is to provide the required DC link voltage depending on the operating speed of the machine. If machine speed is high, required DC link voltage will be high. However, less V_{dc} is demanded to drive the motor at reduced speed. However, due to maximum V_{dc} application even at lower speed could result in more inverter and machine losses. Hence, it is really necessary to calculate appropriate V_{dc} at particular speed. The relationship between V_{dc} and motor speed can be described by following (5).

$$V_{dc} = \sqrt{3}\omega_m P \varphi_s \tag{5}$$

Here, φ_s is the stator flux linkage.

4.1. Calculation of DC-DC converter power stage

4.1.1. Calculation for the buck stage

The (6) is a good approximate equation for calculating minimum value of inductance for buck converter continuous mode operation [22].

$$L_{min} = \frac{V_{out} \times (V_{in} - V_{out})}{\Delta I_L \times f_{sw} \times V_{in}} \tag{6}$$

The output capacitance value for 5% desired voltage ripple can be calculated from the (7) [23].

$$C_{min} = \frac{\Delta I_L}{8 \times f_{sw} \times \Delta V_{out}} \tag{7}$$

4.1.2. Calculation for the boost stage

The (8) is a good approximation for the right inductor for boost mode in a specified range which as follow [24].

$$\text{Ł}_{min} = \frac{V_{in} \times (V_{out} - V_{in})}{\Delta I_L \times f_{sw} \times V_{out}} \tag{8}$$

The output capacitor value for a desired voltage ripple is calculated by the formula (9).

$$C_{min} = \frac{I_{outmax} \times D}{f_{sw} \times \Delta V_{out}} \tag{9}$$

The summary of the key parameters of power converters and PMSM machines which has been considered for simulation are presented in Table 1.

Table 1. Key parameters of PMSM and power converter

Power converter parameters	Value	PMSM machine parameter	Value
Input voltage (V_{in})	100 V	Pole pair (P)	3
Output voltage (V_{dcmax})	160.5 V	Power rating (P_{rated})	1.5 kW
Switching frequency of the DC -DC (f_{sw})	100 kHz	Rated current (I_{rated})	13 A
Switching frequency of the inverter (f_{sw})	16 kHz	Rated speed (N_{rated})	3,000 rpm
Inductor (L_{buck})	342 μH	PM flux of the machine (ψ_m)	0.0852 Wb
Inductor (L_{boost})	502 μH	Torque constant (K_T)	0.383 Nm/A
Output capacitor (C_{buck})	0.2335 μF	Stator resistance (R_s)	0.8434 Ω
Output capacitor (C_{boost})	747μF	d and q axis inductance (L_d=L_q)	1.35 mH

5. RESULTS AND DISCUSSION

The efficiency of the global system and its subsystems (DC-DC converter, three-phase inverter and the motor) are analyzed for both powertrains (C1 and C2) in the form of efficiency maps. Moreover, the efficiency map of the DC-DC converter also discussed. All the efficiency maps data are obtained from the PLECS software using real switches from manufacturers [25].

5.1. Inverter efficiency

The efficiency maps of the inverter for both drivetrain (C1 and C2) is shown in Figure 4 especially in Figures 4(a) dan 4(b). It is observed from the Figure 4(b), that the overall inverter efficiency is significantly improved in topology C2. It can be shown from Figure 4(a), minimum efficiency of inverter has increased from 15.1% to 31.2% whereas maximum efficiency has increased up to 95%. The use of variable V_{dc} control technique is the main reason of this efficiency improvement. Moreover, boost in the efficiency in C2 at lower speed because of less voltage appears across insulated-gate bipolar transistor (IGBTs). Consequently, switching, and conduction losses of the inverter are reduced. Figure 5 illustrates the switching losses in inverter. Particularly, switching losses are reduced due to mainly reduction of magnitude of V_{dc} as shown in Figures 5(a) and 5(a). It is observed from the inverter switching losses maps, at lower speed region, the losses are almost half in C2 with respect to C1 as expected.

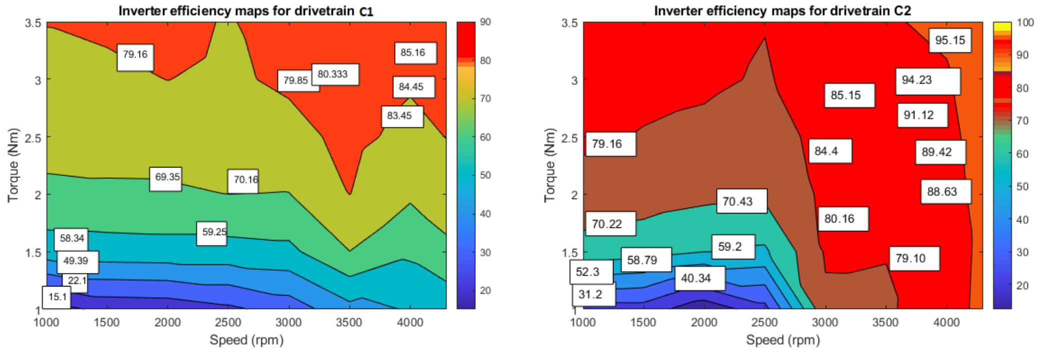

(a) (b)

Figure 4. Inverter efficiency for drivetrain (a) C1 and (b) C2

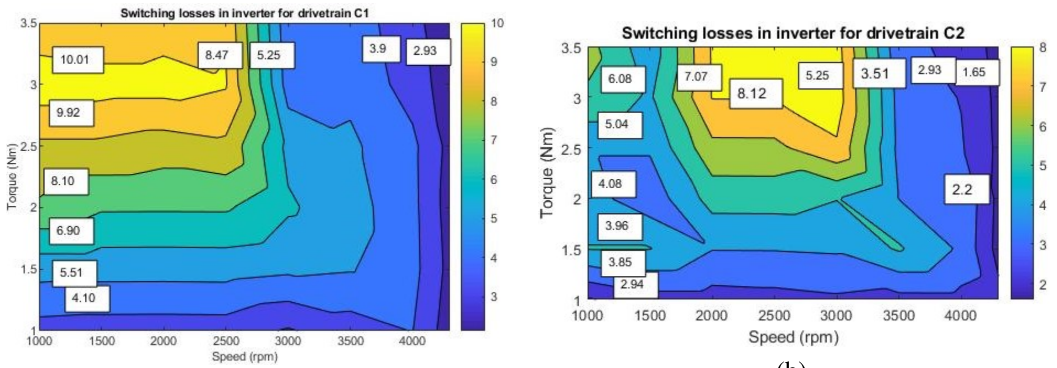

(a) (b)

Figure 5. Switching losses in inverter for drivetrain (a) C1 and (b) C2

5.2. DC-DC converter efficiency

It is noted that the DC-DC converter efficiency changes from 75% to 96% from low speed to high speed region (Figure 6). In addition, with the rise in load torque and motors speed, the efficiency of the system and subsystems increase. The reason behind this is that with the increase in load torque and speed of the motor, the power output from the machine becomes prevalent over the losses.

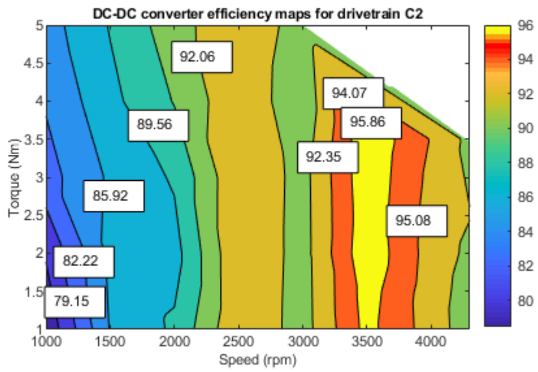

Figure 6. DC-DC converter efficiency map for drivetrain C2

5.3. PMSM motor efficiency map

Figure 7 depicts the PMSM efficiency maps. It is vivid that at the lower speed region efficiency has increased significantly in C2 compared to C1 due to applying of variable V_{dc} control algorithm as shown in Figures 7(a) and 7(b). At reduced speed and load torques, as the inverter controls voltage to the motor through the variable DC link controller, the PMSM voltage is minimized, reducing the iron losses of the motor and thus efficiency improved. The minimum efficiency has increased to 53% from 29% in powertrain C2. However, at high speed and load torque, from Figure 7(a) it is clear that, the efficiency of both configurations (C1 and C2) are almost identical because the voltage of the system is almost the same in that region.

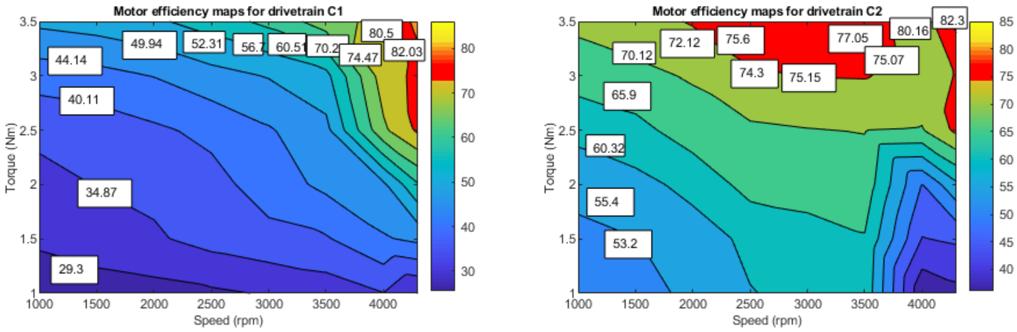

(a) (b)

Figure 7. Motor efficiency for drivetrain (a) C1 and (b) C2

5.4. System efficiency map

Figure 8 presents the overall system efficiency for configurations C1 and C2 respectively. Comparing the outcomes from Figure 8(a) and Figure 8(b), it is found that despite the greater inverter and PMSM efficiency in C2 topology owing to the losses of the DC-DC converter, performance is adversely impacted when PMSM works at elevated speeds and load torque. Thus, taking account only inverter and PMSM losses in drivetrain C1, the system efficiency values of C1 will be higher than C2 configuration at higher speed. However, at the lower speed range, the efficiency of topology C2 becomes higher than C1. This happens because at lower speed V_{dc} control schemes enable system voltage to decrease, leading in lower subsystems losses and thus good efficiency obtained. The minimum efficiency improved in topology C2 is 20% compared to 10% in C1.

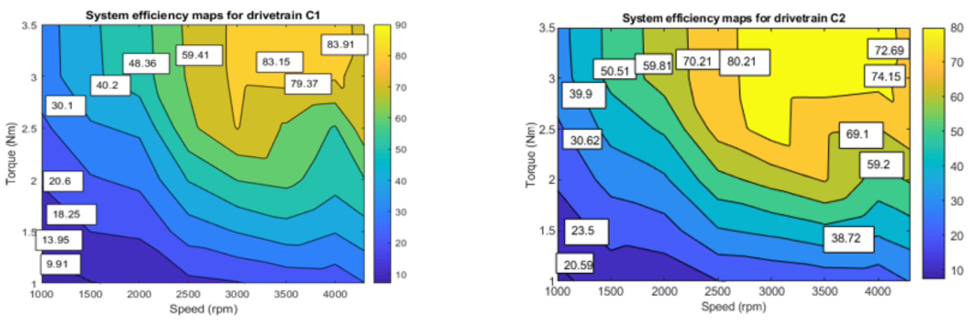

(a) (b)

Figure 8. System efficiency for drivetrain (a) C1 and (b) C2

6. CONCLUSION

The findings obtained from the appearance of efficiency maps offer very effective results on the combinations of torque/speed in which a particular electric drive system is most effective. To sum up, taking in consideration all these factors for an urban driving cycles in which a traction motor most frequently operates at light loads and low speeds, the electric propulsion systems should be designed such that it can provide maximum efficiency and stable performance in this region. Hence, the variable voltage controlled drivetrains fulfill above conditions and well suited for urban driving cycles. However the effects of distortion in PMSM voltage and current directly influence the machine efficiency and lifetime. Hence, total harmonic distortion in voltage and current is needed to be analysed for both C1 and C2 topology in order to have better performance of the drive systems.

REFERENCES

[1] A. Y. Saber and G. K. Venayagamoorthy, "Plug-in vehicles and renewable energy sources for cost and emission reductions," *IEEE Transactions on Industrial Electronics*, vol. 58, no. 4, pp. 1229–1238, Apr. 2011, doi: 10.1109/TIE.2010.2047828.

[2] W. R. Black, *Sustainable transportation: problems and solutions*. The Guilford Press, 2010.

[3] Governor's Office of Planning and Research "Governor's interagency working group on zero-emission vehicles: 'ZEV zero-emission vehicles on California roadways by 2025'," 2016.

[4] S. S. Rao and D. Rangaswamy, "Power quality mitigation and transient analysis in AC/DC hybrid microgrid for electric vehicle charging," *Indonesian Journal of Electrical Engineering and Computer Science (IJEECS)*, vol. 24, no. 3, pp. 1315–1322, Dec. 2021, doi: 10.11591/ijeecs.v24.i3.pp1315-1322.

[5] I. N. Jiya, N. Gurusinghe, and R. Gouws, "Hybridisation of battery, supercapacitor and hybrid capacitor for load applications with high crest factors: a case study of electric vehicles," *Indonesian Journal of Electrical Engineering and Computer Science (IJEECS)*, vol. 16, no. 2, pp. 614–622, Nov. 2019, doi: 10.11591/ijeecs.v16.i2.pp614-622.

[6] D. Hall, M. Moultak, and N. Lutsey, "Electric vehicle capitals of the world: demonstrating the path to electric drive," 2017. [Online]. Available: https://www.theicct.org/sites/default/files/publications/Global-EV-Capitals_White-Paper_06032017_vF.pdf.

[7] M. Zeraoulia, M. E. H. Benbouzid, and D. Diallo, "Electric motor drive selection issues for HEV propulsion systems: a comparative study," *IEEE Transactions on Vehicular Technology*, vol. 55, no. 6, pp. 1756–1764, Nov. 2006, doi: 10.1109/TVT.2006.878719.

[8] J. G. W. West, "DC, induction, reluctance and PM motors for electric vehicles," *Power Engineering Journal*, vol. 8, no. 2, pp. 77–88, Apr. 1994, doi: 10.1049/pe:19940203.

[9] V. T. Buyukdegirmenci, A. M. Bazzi, and P. T. Krein, "Evaluation of induction and permanent-magnet synchronous machines using drive-cycle energy and loss minimization in traction applications," *IEEE Transactions on Industry Applications*, vol. 50, no. 1, pp. 395–403, Jan. 2014, doi: 10.1109/TIA.2013.2266352.

[10] K. M. Rahman, B. Fahimi, G. Suresh, A. V. Rajarathnam, and M. Ehsani, "Advantages of switched reluctance motor applications to EV and HEV: design and control issues," *IEEE Transactions on Industry Applications*, vol. 36, no. 1, pp. 111–121, 2000, doi: 10.1109/28.821805.

[11] D. Casadei, F. Profumo, G. Serra, and A. Tani, "FOC and DTC: two viable schemes for induction motors torque control," *IEEE Transactions on Power Electronics*, vol. 17, no. 5, pp. 779–787, Sep. 2002, doi: 10.1109/TPEL.2002.802183.

[12] K. K. Prabhakar, U. R. Chinthakunta, A. K. Singh, and P. Kumar, "Efficiency and performance analysis of DTC-based IM drivetrain using variable DC-link voltage for electric vehicle applications," *IET Electrical Systems in Transportation*, vol. 8, no. 3, pp. 205–214, Sep. 2018, doi: 10.1049/iet-est.2017.0086.

[13] T. Schoenen, M. S. Kunter, M. D. Hennen, and R. W. D. Doncker, "Advantages of a variable DC-link voltage by using a DC-DC converter in hybrid-electric vehicles," in *2010 IEEE Vehicle Power and Propulsion Conference*, Sep. 2010, pp. 1–5, doi: 10.1109/VPPC.2010.5729003.

[14] R. M. Schupbach and J. C. Balda, "Comparing DC-DC converters for power management in hybrid electric vehicles," in *IEEE International Electric Machines and Drives Conference*, 2003. IEMDC'03., vol. 3, pp. 1369–1374, doi: 10.1109/IEMDC.2003.1210630.

[15] J. O. Estima and A. J. M. Cardoso, "Efficiency analysis of drive train topologies applied to electric/hybrid vehicles," *IEEE Transactions on Vehicular Technology*, vol. 61, no. 3, pp. 1021–1031, Mar. 2012, doi: 10.1109/TVT.2012.2186993.

[16] R. Thumma, V. V. S. K. Bhajana, and P. K. Aylapogu, "Design and simulation of a new ZVT Bi-directional DC-DC converter for electric vehicles," *Indonesian Journal of Electrical Engineering and Computer Science (IJEECS)*, vol. 7, no. 1, pp. 75–83, Jul. 2017, doi: 10.11591/ijeecs.v7.i1.pp75-83.

[17] S. Dusmez, A. Hasanzadeh, and A. Khaligh, "Comparative analysis of bidirectional three-level DC–DC converter for automotive applications," *IEEE Transactions on Industrial Electronics*, vol. 62, no. 5, pp. 3305–3315, May 2015, doi: 10.1109/TIE.2014.2336605.

[18] D. Han, J. Noppakunkajorn, and B. Sarlioglu, "Comprehensive efficiency, weight, and volume comparison of SiC- and Si-based bidirectional DC–DC converters for hybrid electric vehicles," *IEEE Transactions on Vehicular Technology*, vol. 63, no. 7, pp. 3001–3010, Sep. 2014, doi: 10.1109/TVT.2014.2323193.

[19] C.-Y. Yu, J. Tamura, and R. D. Lorenz, "Optimum DC bus voltage analysis and calculation method for inverters/motors with variable DC bus voltage," *IEEE Transactions on Industry Applications*, vol. 49, no. 6, pp. 2619–2627, Nov. 2013, doi: 10.1109/TIA.2013.2265873.

[20] K. K. Prabhakar, M. Ramesh, A. Dalal, C. U. Reddy, A. K. Singh, and P. Kumar, "Efficiency investigation for electric vehicle powertrain with variable DC-link bus voltage," in *IECON 2016 - 42nd Annual Conference of the IEEE Industrial Electronics Society*, Oct. 2016, pp. 1796–1801, doi: 10.1109/IECON.2016.7793714.

[21] P. Sarkar and S. Bhunia, "SVPWM based vector control of PMSM drive in delta domain," in *2017 International Conference on Electrical, Computer and Communication Engineering (ECCE)*, Feb. 2017, pp. 5–10, doi: 10.1109/ECACE.2017.7912869.

[22] B. Hauke, "Basic calculation of a buck converter's power stage," 2015. [Online]. Available: http://www.ti.com/lit/an/slva477b/slva477b.pdf.

[23] M. K. Kazimierczuk, *Pulse-width modulated DC-DC power converters*, 2nd ed. Wiley, 2015.

[24] "Buck-boost converter using the STM32F334 discovery kit," 2014. [Online]. Available: https://www.st.com/en/evaluation-tools/32f3348discovery.html.

[25] "Low loss IGBT: IGBT in TRENCHSTOPTM and fieldstop technology." 2015. [Online]. Available: https://www.infineon.com/dgdl/Infineon-IGP15N60T-DS-v02_04-EN.pdf?fileId=db3a30432313ff5e0123b84fabee78ad.

BIOGRAPHIES OF AUTHORS

Muhammad Helal Uddin is assistant professor at Department of Electrical and Electronic Engineering, Premier University, Bangladesh. He received the B.Sc. in Electrical and Electronic Engineering from Chittagong University of Engineering and Technology (CUET) and M.Sc. in sustainable transportation and electrical power systems from University of Oviedo, Spain. His research areas are control of machines and power converters applied for different applications, microgrid modeling, and FACTS controller. He can be contacted at email: helal_eee@puc.ac.bd.

Sharith Dhar is lecturer at Department of Electrical and Electronic Engineering, Premier University, Bangladesh. He received the B.Sc. in Electrical and Electronic Engineering from Premier University, Bangladesh. His research areas are AC machine control, machine learning, and renewable energy optimization. He can be contacted at email: sharithdhar@gmail.com.

Asif Mohammed Siddiqee is lecturer at Department of Electrical and Electronic Engineering, Premier University, Bangladesh. He received the B.Sc. in electrical and and electronic engineering from Chittagong University of Engineering and Technology (CUET). His research areas are machine learning, power system optimization, and microwave antenna. He can be contacted at email: asifuseee@gmail.com.

Rahul Chowdhury is lecturer at Department of Electrical and Electronic Engineering, Premier University, Bangladesh. He received the B.Sc. in electrical and and electronic engineering from Chittagong University of Engineering and Technology (CUET). His research areas are power electronic devices, power system optimization, and renewable energy. He can be contacted at email: rahul.cuet.eee@gmail.com.

Akramul Haque is assistant professor at Department of Electrical and Electronic Engineering, Premier University, Bangladesh. He received the B.Sc. and M.Sc. in electrical and and electronic engineering from Chittagong University of Engineering and Technology (CUET). His research areas are micro grid including different distributed energy sources (DESs) like: photovoltaic farm, wind farm, and battery storages. He can be contacted at email: akramul073@gmail.com.

Mohammed Saifuddin Munna is assistant professor at Department of Electrical and Electronic Engineering, Premier University, Bangladesh. He received the B.Sc. in electrical and electronic engineering from Premier University, Bangladesh. His research areas are power systems, machine learning, and renewable energy. He can be contacted at email: munna.puc@gmail.com.